Electronic Supplementary Material (ESI) for Journal of Materials Chemistry C.

Supporting Information

for

On the Interaction Between Up-converting $NaYF_4:Er^{3+},Yb^{3+}$ Nanoparticles and Rose Bengal Molecules Constrained within the Double Core of Mulifunctional Nanocarriers

Dominika Wawrzyńczyk[a,*], Bartłomiej Cichy[b], Jan K. Zaręba[a] and Urszula Bazylińska[c,*]

[a]Advanced Materials Engineering and Modelling Group, Faculty of Chemistry, Wroclaw University of Science and Technology, Wybrzeze Wyspianskiego 27, 50-370 Wroclaw, Poland

[b]Institute of Low Temperature and Structure Research Polish Academy of Sciences, Okólna 2, 50-422 Wroclaw, Poland

[c]Faculty of Chemistry, Wroclaw University of Science and Technology, Wybrzeze Wyspianskiego 27, 50-370 Wroclaw, Poland

[*]corresponding authors: dominika.wawrzynczyk@pwr.edu.pl, urszula.bazylinska@pwr.edu.pl

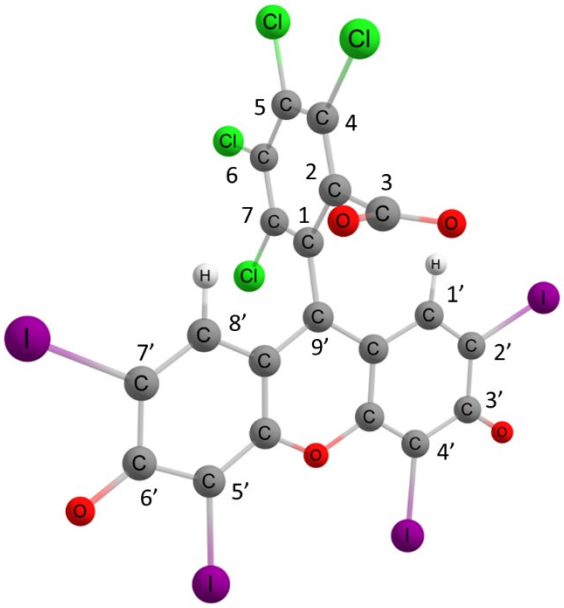

Figure S1. Optimized geometry of model form of Bengal Rose molecule that is considered in this work. For purpose of the calculations C(1') and C(8') atoms were saturated by hydrogen atoms. Meaning of the color spheres goes as follows: purple spheres - iodine atoms (7',5',4',2'), red spheres – oxygen, green spheres – chloride atoms (4,5,6,7) and gray spheres represent carbon atoms.

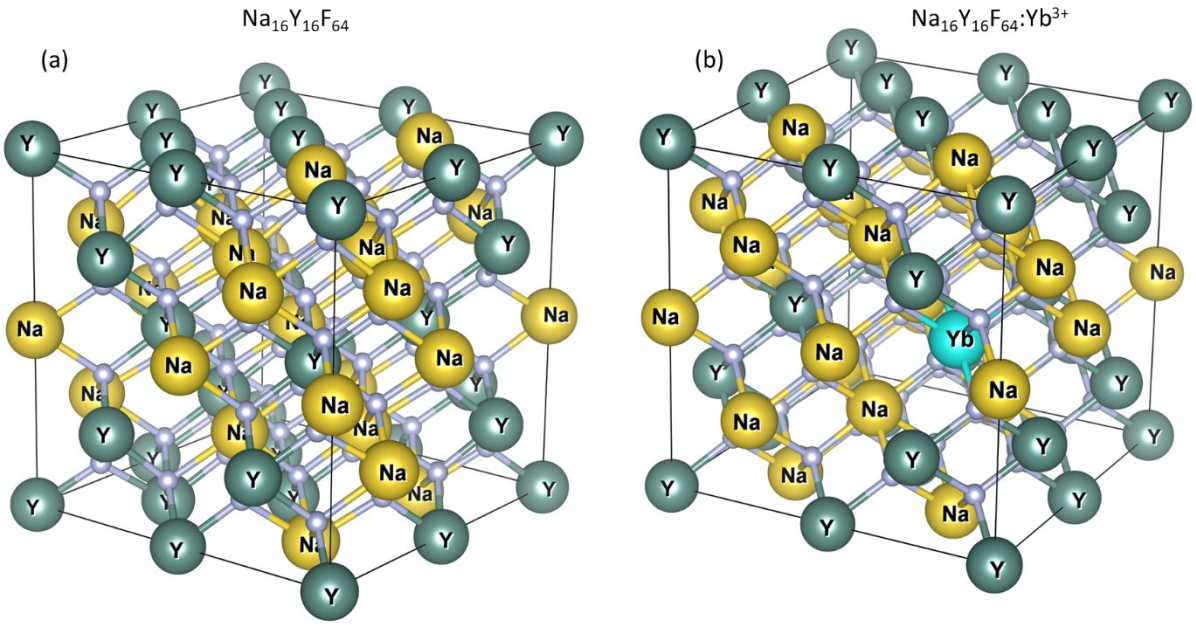

Figure S2. The $Na_{16}Y_{16}F_{64}$ supercell (a) and $Na_{16}Y_{16}F_{64}$ supercell doped with Yb^{3+} (b) used for the DFT calculations. The Yb was exchanged with an Y atom.

Table S1. Structural parameters for the $Na_{16}Y_{16}F_{64}$ the $Na_{16}Y_{16}F_{64}$:Yb supercell models obtained from geometry optimization with the DFT formalism compared with corresponding parameters calculated based on Rietveld refinement of measured XRD diffraction pattern of synthesized $NaYF_4$:Er^{3+},Yb^{3+} NPs.

	$Na_{16}Y_{16}F_{64}$ (DFT calculations)	$Na_{16}Y_{16}F_{64}$ (DFT calculations)	$NaYF_4$ (experimental)
Cell parameters (Ang.):			
a	9.783064	9.761690	5.521
b	9.830707	9.966607	5.521
c	9.783999	9.898127	5.521
Cell angles (deg.):			
Alpha	90.0199	90.2368	90
Beta	90.0382	89.8621	90
Gamma	90.0568	89.9166	90
Cell volume ($Ang.^3$):	940.9700	962.9860	168.288
Atomic forces (eV/Ang.):	0.039374	0.037178	-

Table S2. Characteristics of PEG-HA-NCs loaded by $NaYF_4:Er^{3+},Yb^{3+}$ NPs and different concentration of RB obtained by nanoemulsion structural design (a double emulsion and layering) methods.

Sample	C_{RB} (μM)	D_H (nm)	PdI	ζ (mV)
1	0	127±2	0.26±0.02	-2±1
2	50	134±3	0.28±0.02	-4±1
3	100	143±4	0.29±0.03	-4±1
4	250	151±5	0.28±0.02	-3±1
5	350	150±5	0.29±0.03	-4±1
6	500	152±5	0.31±0.03	-3±1
7	700	154±5	0.30±0.03	-3±1

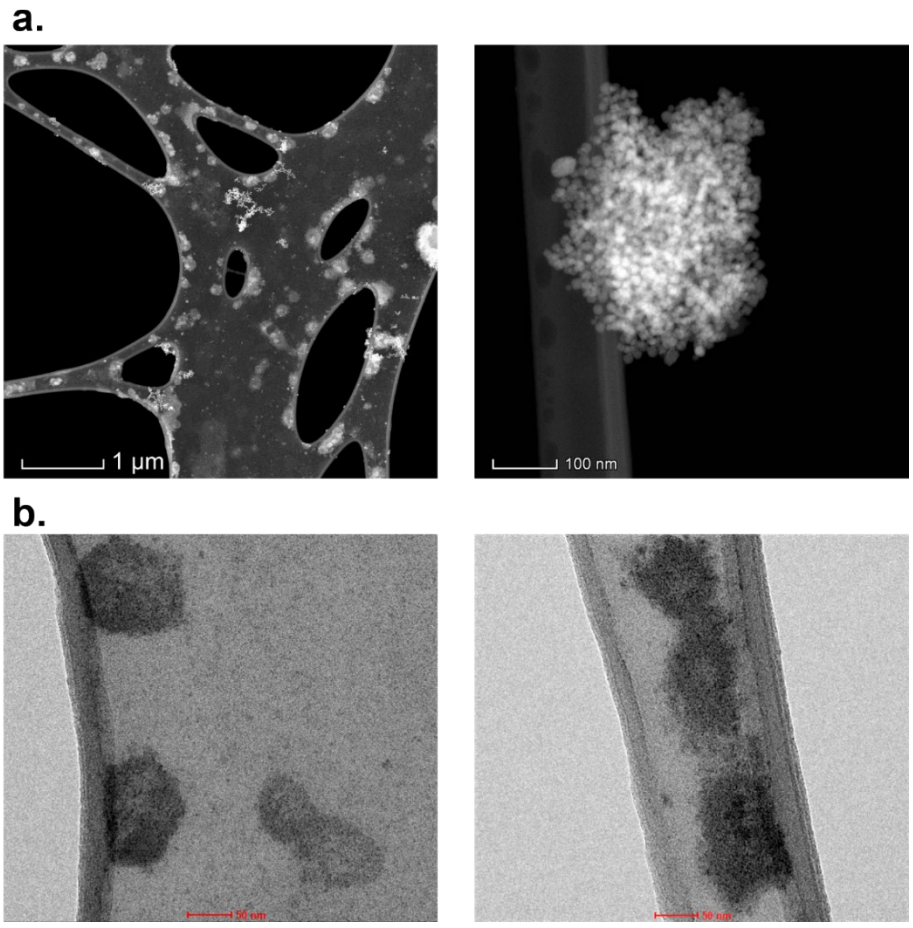

Figure S3. HAADF-STEM (a) and bright field (b) TEM images of the co-loaded NCs.

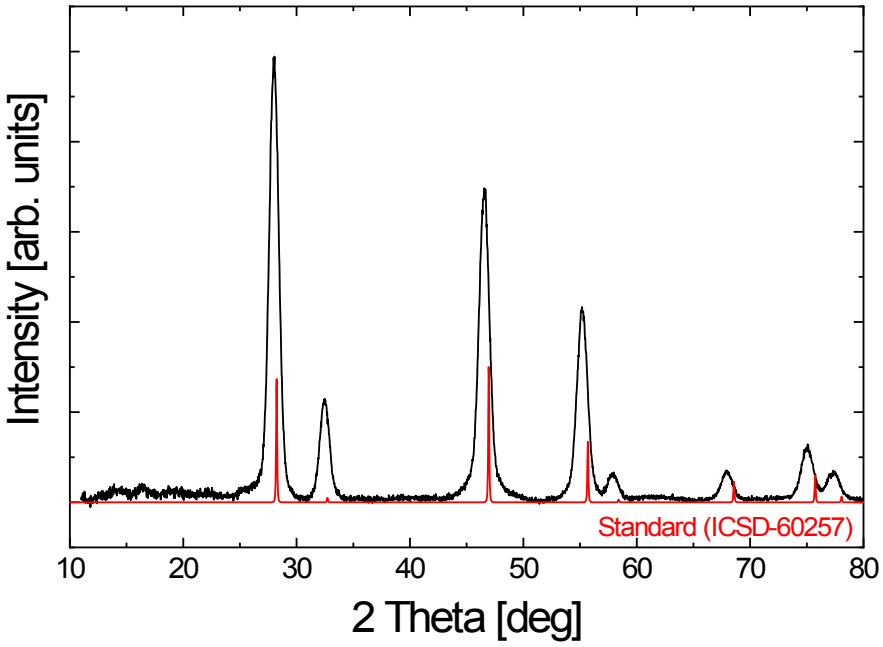

Figure S4. XRD powder diffraction pattern measured for the as-synthesized $NaYF_4:Er^{3+},Yb^{3+}$ NPs and compared with the standard (ICSD-60257) pattern for the cubic $NaYF_4$ matrix.

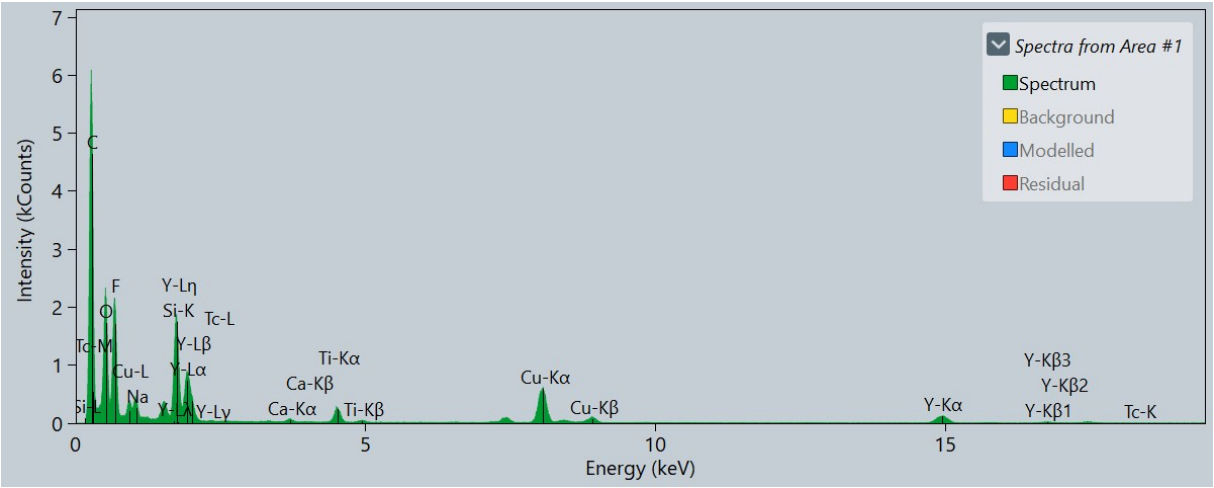

Figure S5. EDS analysis of the composition, microstructure, and atomic structure of the materials used for the NCs preparation.

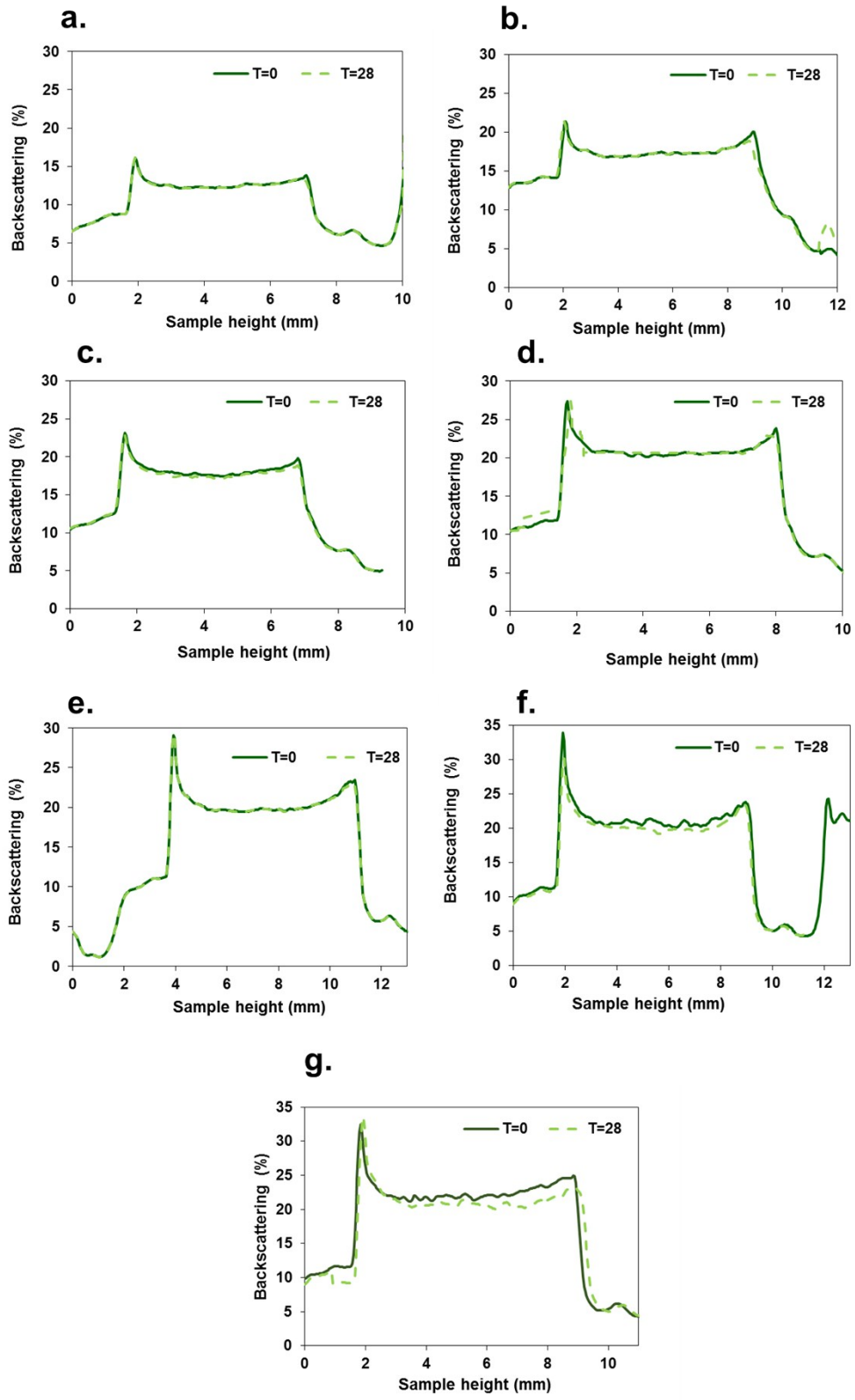

Figure S6. Backscattering profiles of the various PEG-HA NCs co-loaded by $NaYF_4:Er^{3+},Yb^{3+}$ NPs and RB molecules as a function of sample height (mm) analyzed over 28 days of the NCs storage. (see descriptions for the systems 1−7 in Tab. S1).

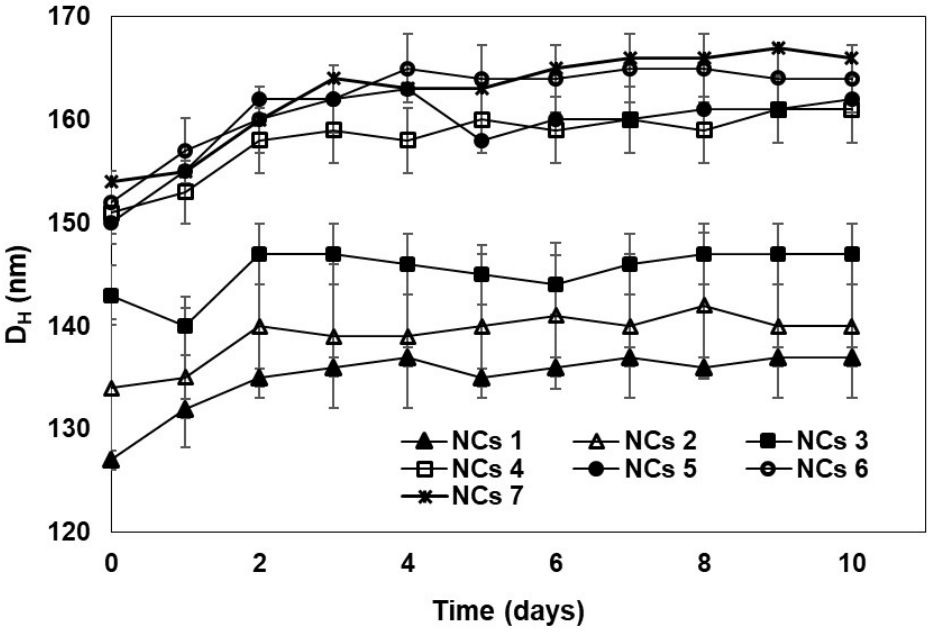

Figure S7. Time-dependent measurements of hydrodynamic diameter (D_H) for the nanosystems incubated in 10%FBS in DMEM (see descriptions for the systems 1−7 in Tab. S1).

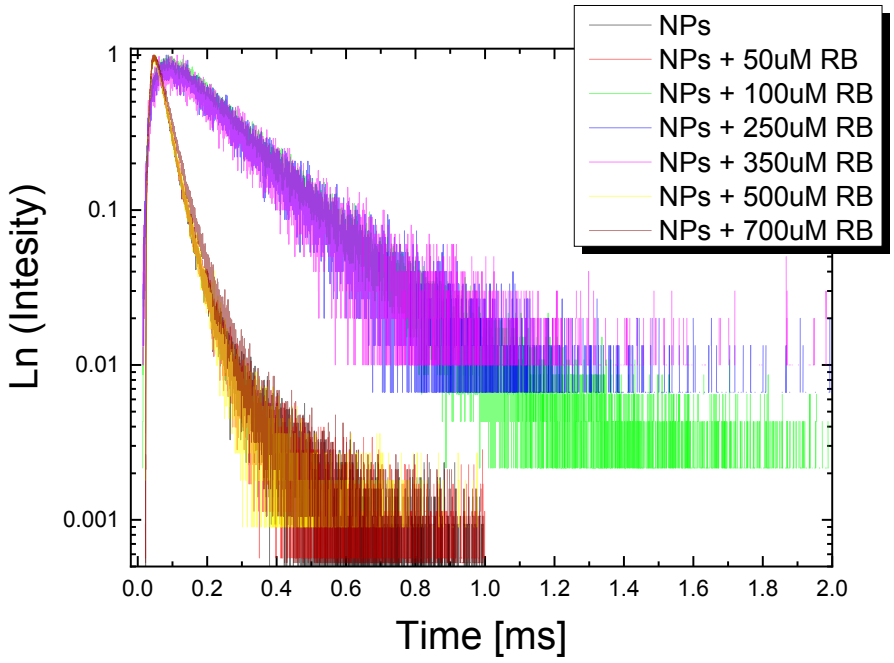

Figure S8. Luminescence decay curves measured at 540 nm ($^2H_{11/2} + {}^4S_{3/2} \rightarrow {}^4I_{15/2}$ transition) upon 980 nm excitation for NCs loaded with only $NaYF_4:Er^{3+},Yb^{3+}$ NPs and with co-encapsulated increasing amounts of RB.

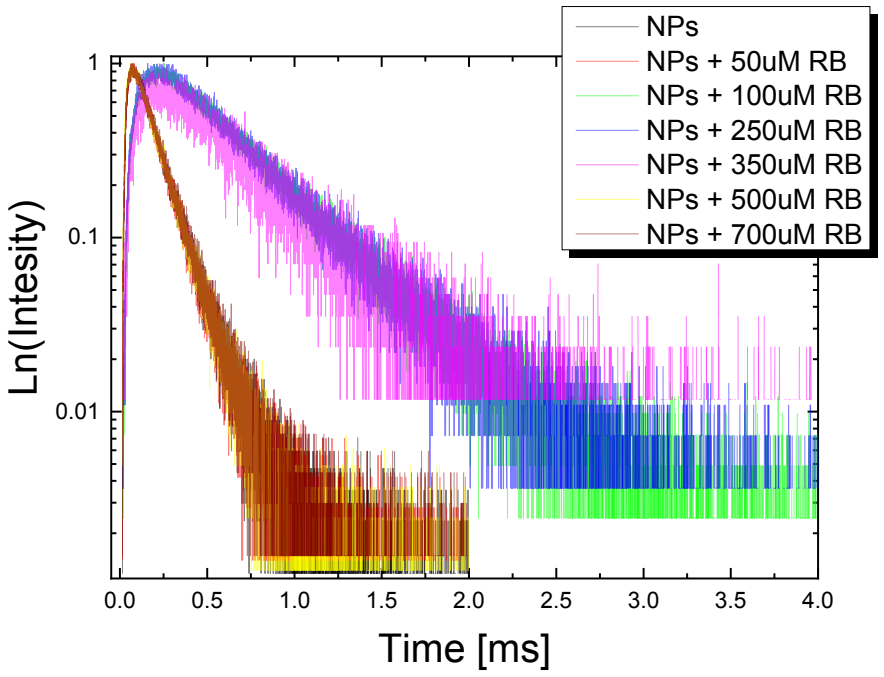

Figure S9. Luminescence decay curves measured at 660 nm ($^4F_{9/2} \rightarrow {}^4I_{15/2}$ transition) upon 980 nm excitation for NCs loaded with only $NaYF_4:Er^{3+},Yb^{3+}$ NPs and with co-encapsulated increasing amounts of RB.

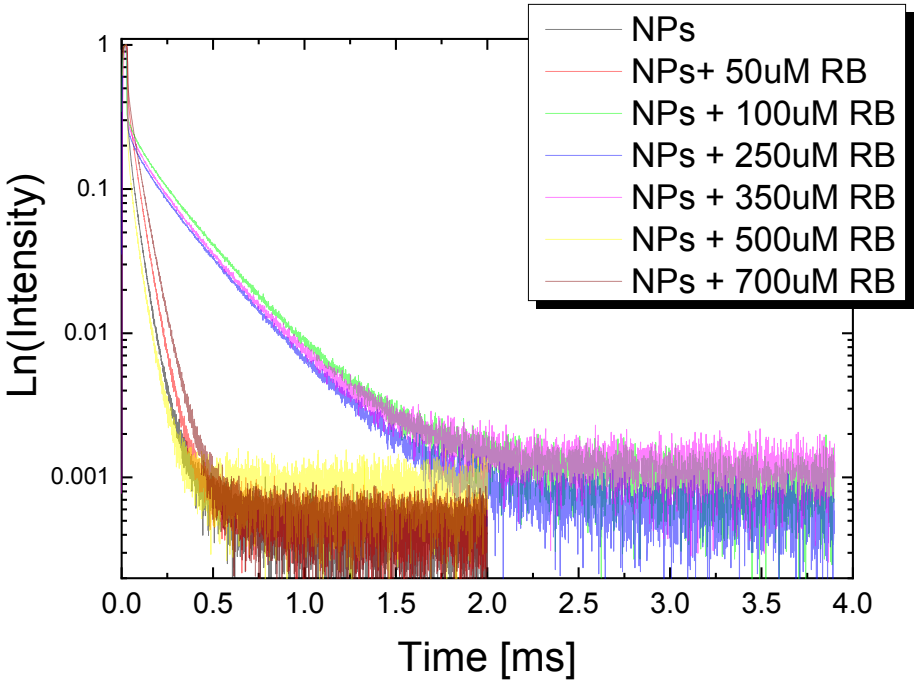

Figure S10. Luminescence decay curves measured at 1030 nm ($^2F_{5/2} \rightarrow {}^2F_{7/2}$ transition) upon 980 nm excitation for NCs loaded with only $NaYF_4:Er^{3+},Yb^{3+}$ NPs and with co-encapsulated increasing amounts of RB.

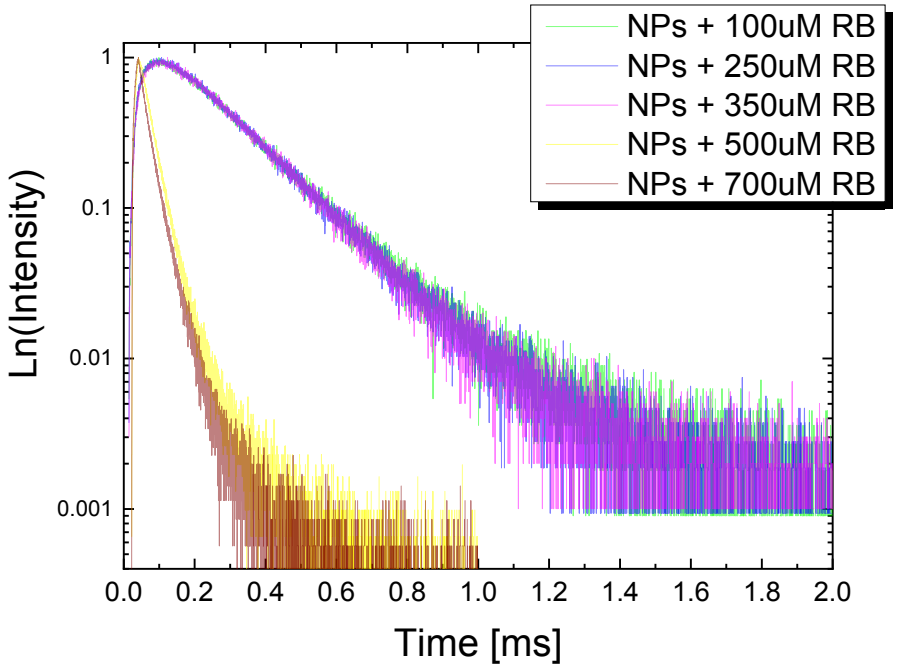

Figure S11. Luminescence decay curves of RB emission at 600 nm observed upon 980 nm excitation measured for NCs loaded with $NaYF_4:Er^{3+},Yb^{3+}$ NPs and increasing amounts of RB.

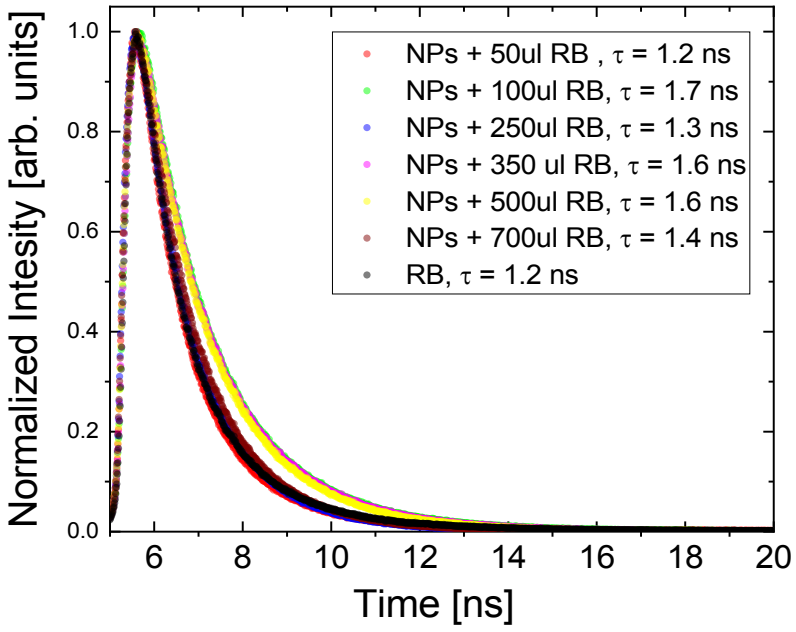

Figure S12. Luminescence decay curves of RB emission at 600 nm observed upon direct 516 nm excitation measured with the TCSPC technique for NCs loaded with $NaYF_4:Er^{3+},Yb^{3+}$ NPs and increasing amounts of RB.

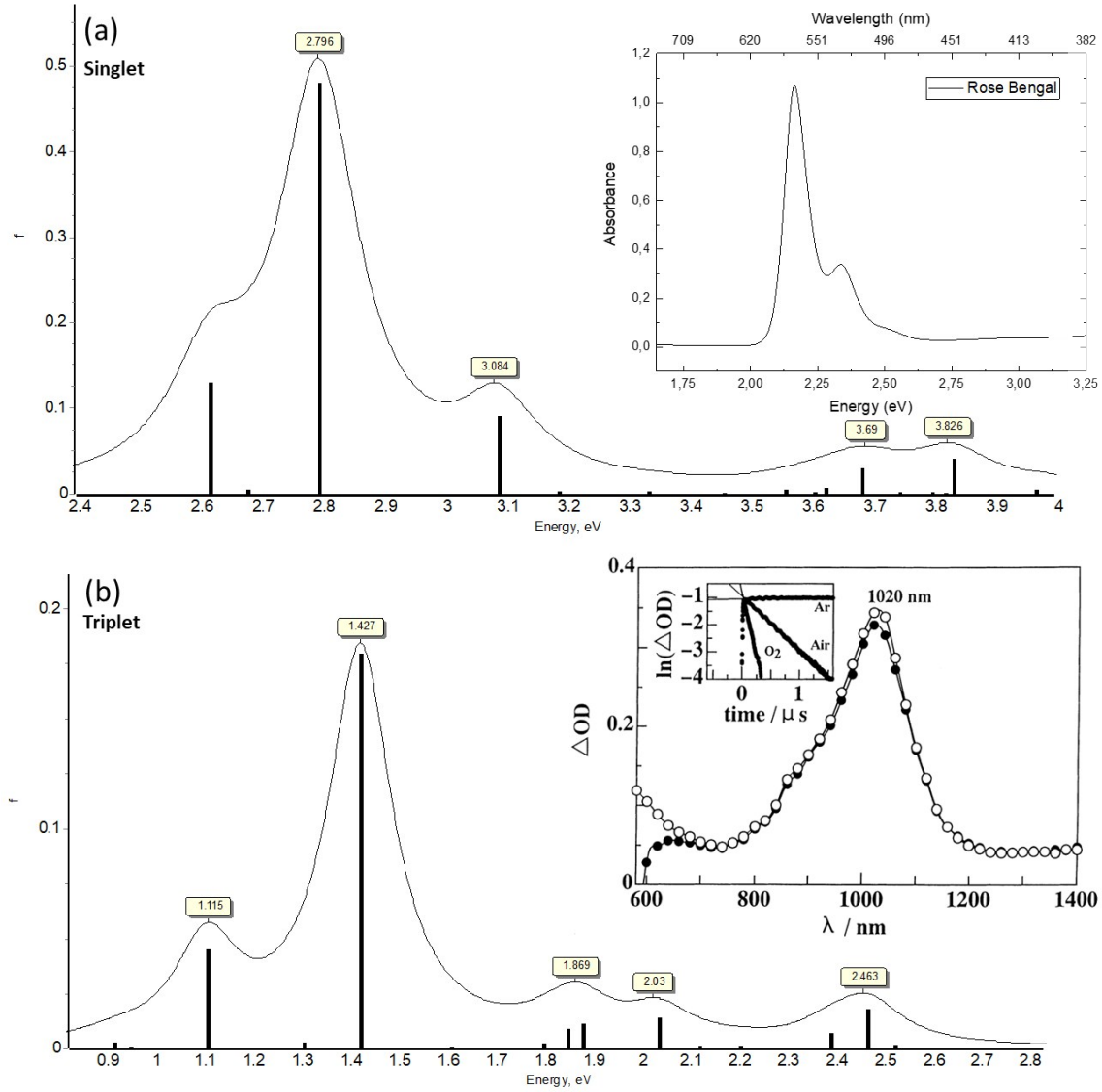

Figure S13. Dispersion of the oscillator strength for electronic transitions in RB molecule calculated for (a) singlet state compared with the measured absorption spectra (insert), and (b) triplet state configuration compared with experimentally measured transient absorption spectra of this transition – insert in (b) was taken from [Journal of Photochemistry and Photobiology A: Chemistry 123 (1999) 53 – 59].

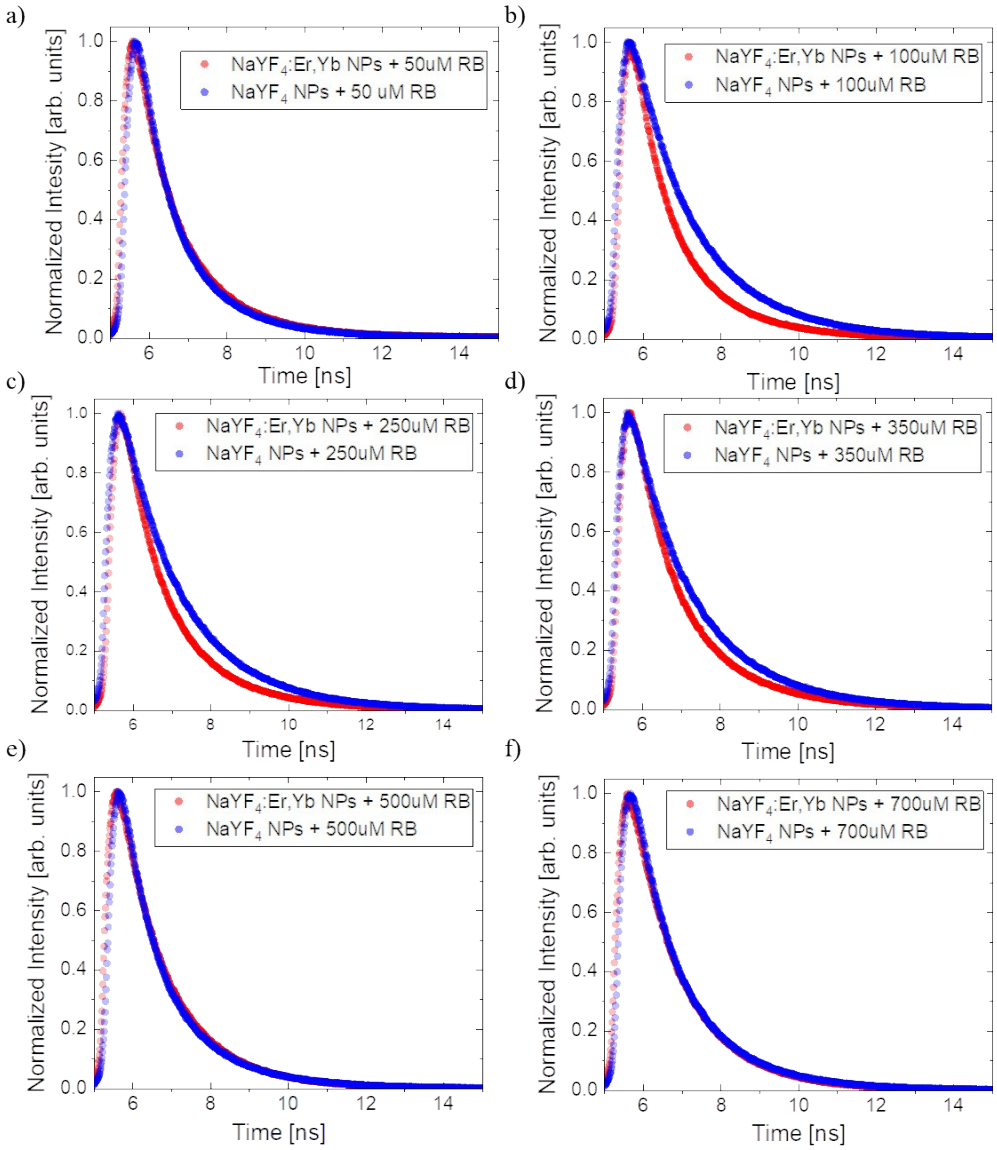

Figure S14. Luminescence decay curves of RB emission at 600 nm observed upon direct 516 nm excitation measured with the TCSPC technique for NCs loaded with $NaYF_4:Er^{3+},Yb^{3+}$ NPs (red dots), un-doped $NaYF_4$ NPs (blue dots) and increasing amounts of RB.

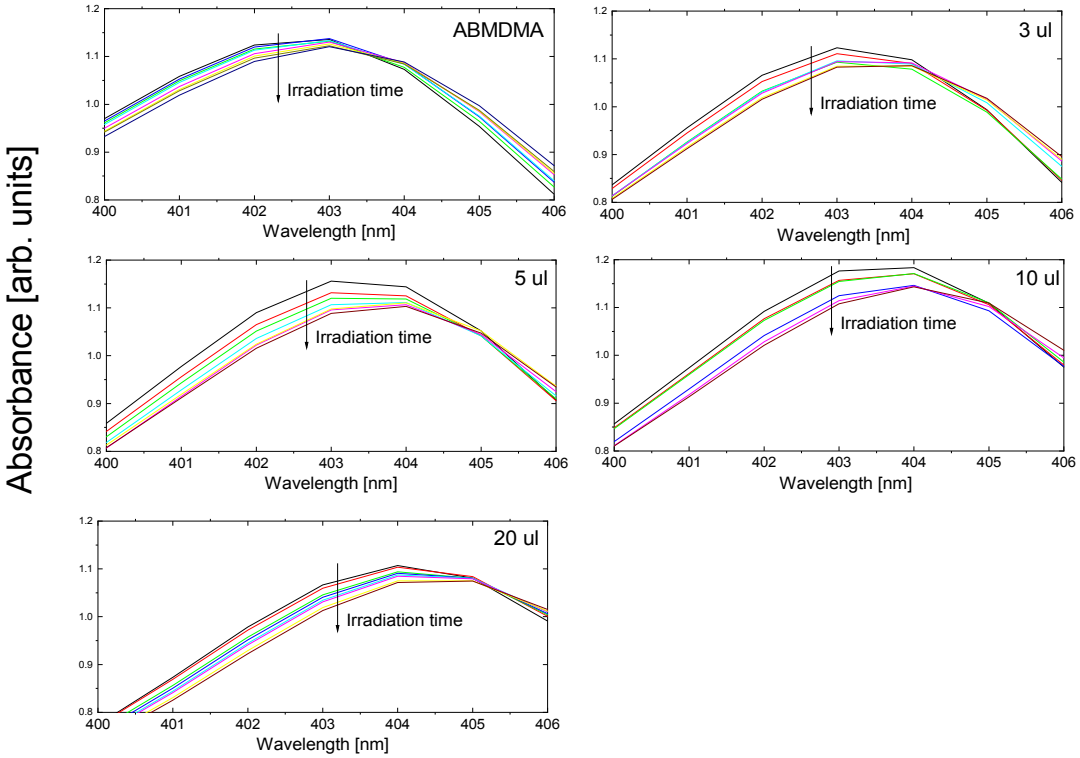

Figure S15. The changes in absorption spectra of ABMDMA solution without, and with added different amounts of $NaYF_4:Er^{3+},Yb^{3+}$ NPs and RB molecules congaing NCs measured as a function of 980 nm laser diode irradiation times.

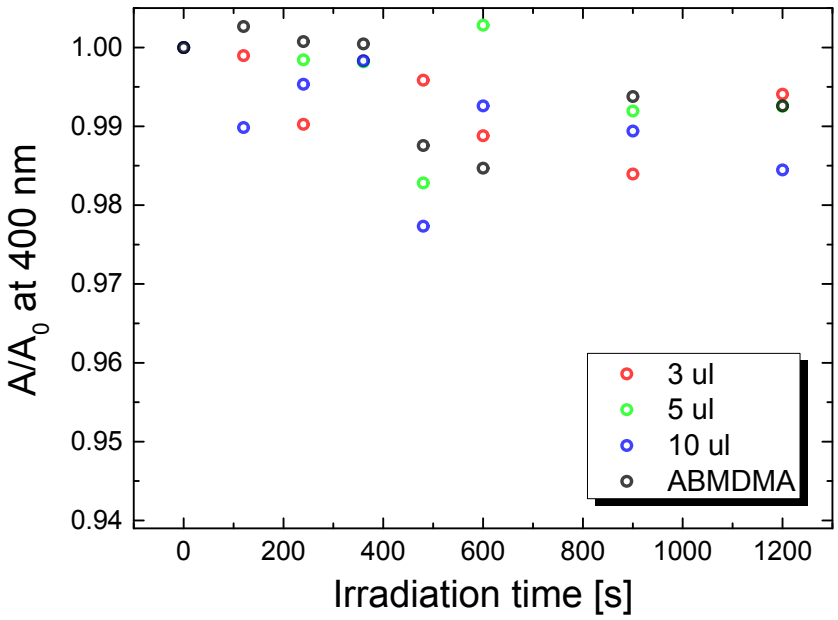

Figure S16. Photobleaching of ABMDMA by singlet oxygen generated in a presence of NCs loaded with $NaYF_4:Er^{3+},Yb^{3+}$ NPs and 250 μM of RB, the change in ABMDMA absorption at 400 nm was measured as a function of 980 nm laser diode irradiation time and the amount of added NCs to the solution.

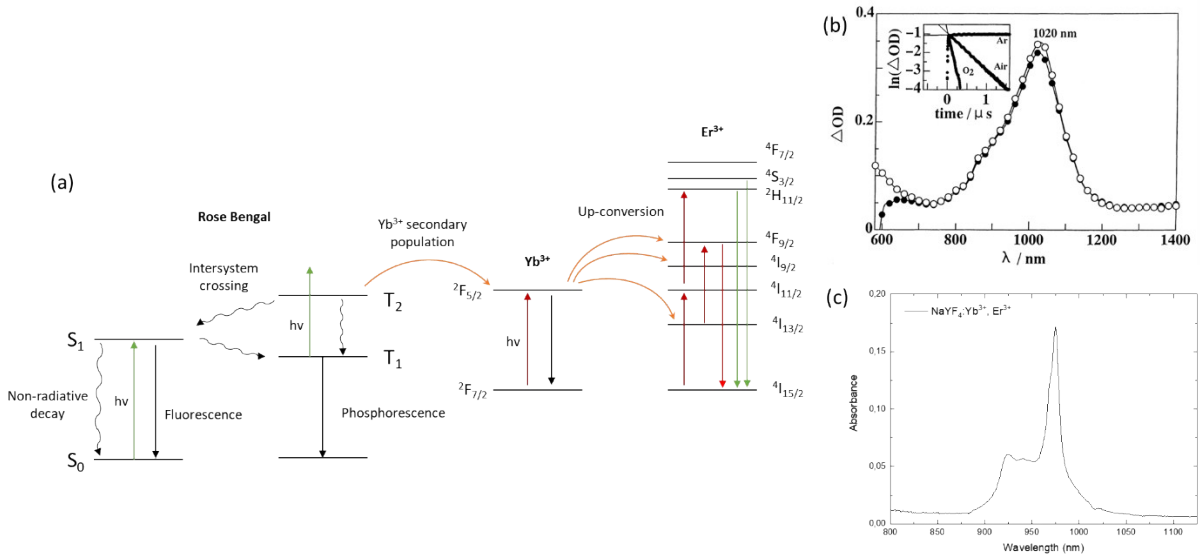

Figure S17. Proposed Jablonski diagram for RB molecule and $NaYF_4:Yb^{3+}$, Er^{3+} NPs showing the possible pathways of energy transfer processes (a). Transient absorption spectra of RB molecules, dissolved in deareated ethanol, after excitation with 532 nm (b). Black and white circles depicts spectra at probe delay of 0.1 us and 1 us, respectively. Inset depicts decay curves of the T-T transition. Figure (b) was taken from [Journal of Photochemistry and Photobiology A: Chemistry 123 (1999) 53 – 59]. Absorbance band of Yb^{3+} ions of the $NaYF_4:Yb^{3+}$, Er^{3+} NPs (c).